Lifting-Line Theory of Oblique Wings

H. K. Cheng*
University of Southern California, Los Angeles, Calif.

Introduction

THE analysis of far-wake vorticity effect is essential in the problem of three-dimensional lifting surfaces. This task is greatly simplified in Prandtl's lifting-line theory in which the bound vortices on the wing are replaced by a line of singularity.[1] A restriction in Prandtl's work, as well as the more systematic, asymptotic theory[2,3] is that the wing centerline (a reference curve in the theory) is required to be straight and unswept (being perpendicular to the main flow). The present study considers extensions of this approach to planar wings involving swept and curved centerlines. Oscillating high-aspect-ratio wings with curved centerlines have been treated by the author in Ref. 4; however, upwash calculation for the low-frequency and quasisteady cases were not given, and the formal inner solution presented therein is incomplete (see following). The primary purpose of this Note is to bring out certain distinct features of such a theory, concentrating on the development for an oblique wing in a steady incompressible potential flow (of which the centerline may be taken as being straight). A comparison with exact solutions and results from other methods will be made. A fuller version of this work is found in Ref. 5. Extensions to oblique wings with transonic component flow[6] and to planforms with curved centerlines in the steady and unsteady cases are treated in separate works.

In the following analysis, two right-handed Cartesian systems are used. The (x,y,z) system is one with the x axis parallel to the freestream and the z axis along the lift direction. The second system (x',y',z') is generated from the first by a rotation about the z axis (Fig. 1).

$$x'=\cos\Lambda x-\sin\Lambda y,\quad y'=\sin\Lambda x+\cos\Lambda y,\quad z'=z \tag{1}$$

Note that the wing plane lies in $z=z'=0$, and that Λ is the sweep angle. Variables x' and z' will be normalized by the root chord c_0 (measured along the x' axis); y', along with x,y, and z, normalized by the half-span b. The primed system is employed to describe the inner region near the wing section and the unprimed one for the outer region. The analysis will employ an aspect ratio $\mathcal{R}_1\equiv 2b/c_0$; later, an aspect ratio based on unyawed quantities $\mathcal{R}_0\equiv 2\ell/c_0=\mathcal{R}_1\sec\Lambda$ is also used, where 2ℓ is the distance from tip to tip. Let the freestream velocity be U, and the parameter controlling camber and incidence be ϵ. The wing (camber surface) ordinate z_w, normalized by ϵc_0, is written as $Z(x',y')$.

The perturbation potential ϕ of the full linearized problem must satisfy the Laplace equation in x,y, and z, being regular everywhere except in approaching the wing and the trailing vortex sheet; it must also vanish at infinity except near the far wake. In approaching the wing, the impermeability condition (applied to upper and lower surfaces) is

$$(\partial\phi/\partial z)_w=U\partial z_w/\partial x \tag{2a}$$

and in approaching the trailing vortex (TV) sheet, the continuity of pressure and normal velocity requires

Received April 12, 1978; revision received Aug. 14, 1978.

Index categories: Subsonic Flow; Transonic Flow; Aerodynamics.

*Professor, Dept. of Aerospace Engineering. Member AIAA.

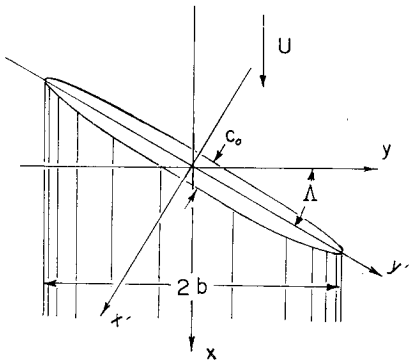

Fig. 1 Two coordinate systems and characteristic length scales.

$$[\![\,\partial\phi/\partial x\,]\!]_{TV}=[\![\,\partial\phi/\partial z\,]\!]_{TV}=0 \tag{2b}$$

where the subscripts w and TV signify the wing and the trailing-vortex sheet, respectively, and the double bracket $[\![\ ]\!]$ stands for differences across the wing or the TV sheet. The velocity is allowed to be unbounded at the leading edge but must be integrable; the pressure or ϕ_x on the wing is required to remain bounded at the trailing edge so that the Kutta condition is satisfied.

Inner Problem

The linearized problem under a small ϵ admits a development for high aspect ratio (for finite x',y',z')

$$\phi'\equiv\phi/\epsilon c_0 U\cos\Lambda=\phi_0+\mathcal{R}_1^{-1}\phi_1+\mathcal{R}_1^{-2}\phi_2+\ldots \tag{3}$$

allowing a weak logarithmic dependence of ϕ_1 and ϕ_2 on $\mathcal{R}_1$. The first two terms satisfy the two-dimensional Laplace equation in x' and z'. The conditions on the wing and the vortex sheet, Eqs. (2), through the transform Eq. (1), yield

$$(\partial\phi_0/\partial z')_w=\partial Z/\partial x' \tag{4a}$$

$$[\![\,\partial\phi_0/\partial x'\,]\!]_{TV}=[\![\,\partial\phi_0/\partial z'\,]\!]_{TV}=0 \tag{4b}$$

$$(\partial\phi_1/\partial z')_w=2m\partial Z/\partial y' \tag{5a}$$

$$[\![\,\partial\phi_1/\partial x'\,]\!]_{TV}+2m[\![\,\partial\phi_0/\partial y'\,]\!]_{TV}=[\![\,\partial\phi_1/\partial z'\,]\!]_{TV}=0 \tag{5b}$$

where $m\equiv\tan\Lambda$, and $2m[\![\,\partial\phi_0/\partial y'\,]\!]_{TV}$ results from the component of trailing vorticity parallel to the centerline.

The solution ϕ_0 satisfying conditions of Eqs. (4), fulfilling the edge conditions mentioned, yielding a zero disturbance velocity at large $x'^2+z'^2$, is provided by the classical two-dimensional thin airfoil theory. As is well known, the vorticity strength $[\![\,\partial\phi_0/\partial x'\,]\!]$ on the wing is a solution to the integral equation

$$\frac{1}{2\pi}P.V.\int_{a'}^{b'}[\![\,\partial\phi_0/\partial x'\,]\!]\frac{dx'}{x_1'-x'}=\frac{\partial}{\partial x'}Z,\quad a'<x'<b' \tag{6}$$

where $P.V.$ signifies the Cauchy principal value; a' and b' locate the leading and trailing edges, respectively.

The solution ϕ_1 that meets the same edge singularity requirements and allows matching with the outer solution can be obtained as the sum

$$\phi_1=\varphi+\varphi^P+V_1^\infty z' \tag{7}$$

where V_1^∞ is an anticipated upwash correction to be determined by matching later; φ^P is a (particular) solution satisfying the (nonhomogeneous) TV boundary conditions in Eq. (5b), and φ is a (wakeless) two-dimensional thin airfoil solution with its wing upwash so chosen to make ϕ_1 fulfill Eq.

(5a). The solution φ^P can be obtained as

$$\varphi^P = -2mR.P.(\zeta\partial W/\partial y') + \varphi_H^P \tag{8}$$

where $R.P.$ signifies the real part; ζ is the complex variable $x'+iz'$, W is the complex potential $\phi_0+i\psi_0$; φ_H^P is a wakeless harmonic function (not considered in Ref. 4) needed to keep φ^P, hence ϕ_1, from becoming more singular than ϕ_0 at the edges (see following). To fulfill Eq. (5a), the jump in $\partial\varphi/\partial x'$ across the wing must satisfy the same integral equation as Eq. (6), with the right-hand side replaced, however, by

$$V_1 \equiv 2m\partial Z/\partial y' + 2mx'\partial^2 Z/\partial y'\partial x' - (\partial\varphi_H^P/\partial z')_w + 2m\partial(Z-Z_{LE}-\psi_{0_{LE}})/\partial y' - V_1^\infty \tag{9}$$

In the absence of the Kutta condition, the φ_H^P, together with the part of φ contributed by $-(\partial\varphi_H^P/\partial z')_w$ in V_1 would belong to the family of eigensolutions for ϕ_1.

In choosing φ_H^P, one notes that the singular behavior of ϕ_1 is dominated by the first member of φ^P in Eq. (8) as $2ma'(\partial a'/\partial y')\partial W/\partial\xi$ at the leading edge and $2m'(\partial b'/\partial y')\partial W/\partial\zeta$ at the trailing edge. For cases wherein the camber slope is nowhere infinite, it suffices to take

$$\varphi_H^P = 2ma'\frac{\partial}{\partial y'}\phi_0 + 2m(c')^{1/2}E\frac{\mathrm{d}}{\mathrm{d}y'}b'R.P. \times[i(\zeta-a')^{1/2}(\zeta-b')^{1/2}-i\zeta] \tag{10a}$$

where E is the coefficient in $\partial\phi_0/\partial x' \sim E(b'-x')^{1/2}$. For the case with infinite camber slopes at the edges, the prescription is

$$\varphi_H^P = 2ma'\frac{\partial}{\partial y'}\phi_0^{LE} + 2mb'\frac{\partial}{\partial y'}\phi_0^{TE} \tag{10b}$$

where ϕ_0^{LE} is a solution of the ϕ_0 type, with its x' derivative tending to $\partial\phi_0/\partial x'$ at LE and vanishing no less rapidly than $(b'-x')$ at TE; ϕ_0^{TE} is similar, with superscript LE replaced by TE and a' by b'. An important example for this case is logarithmically infinite cambers supporting finite pressure jumps at the edges.

In terms of the pressure coefficient C_p' based on the dynamic pressure of the component flow, the pressure jump across the wing can be obtained from

$$[\![C_p']\!]/2\epsilon = -\frac{\partial}{\partial x'}[\![\phi_0]\!] - \mathcal{R}_1^{-1}[\![\frac{\partial}{\partial x'}\varphi - 2mx'\frac{\partial^2}{\partial y'\partial x'}\phi_0 + \frac{\partial}{\partial x'}\varphi_H^P]\!] \tag{11}$$

The span loading is $\rho_\infty U$ times the potential jump at the trailing edge at the y (spanwise) station and can be computed from the jumps in ϕ_0, φ, and φ_H^P at the trailing edge at the corresponding y' station; in normalized form

$$SL \equiv 2b\rho_\infty U[\![\phi]\!]_{TE}/\tfrac{1}{2}\rho_\infty U^2 S_w = 4bc_0 S_w^{-1}\epsilon\cos\Lambda[\![\phi_0+\mathcal{R}_1^{-1}(\varphi+\varphi_H^P)]\!]_{TE} \tag{12}$$

In the outer limit $|\zeta|\to\infty$, the inner solution becomes

$$\phi' \sim (2\pi)^{-1}\Pi(y')1[\tan^{-1}\left(\frac{x'}{z'}\right)+\frac{\pi}{2}\mathrm{sgn}z'] - (2\pi)^{-1}\times\int_{a'}^{b'}[\![C_{p_0}']\!]x_1'\mathrm{d}x_1' R.P.(i\zeta^{-1}) + \mathcal{R}_1^{-1}\pi^{-1}m\frac{\mathrm{d}}{\mathrm{d}y'}\Pi_0 z'\ln|\zeta| - \mathcal{R}_1^{-1}\pi^{-1}m\frac{\mathrm{d}}{\mathrm{d}y'}\Pi_0 x'\left[\tan^{-1}\left(\frac{x'}{z'}\right)+\frac{\pi}{2}\mathrm{sgn}z'\right] + \mathcal{R}_1^{-1}V_1^\infty z' + O(z'\zeta^{-1}\mathcal{R}_1^{-1},\mathcal{R}_1^{-2}) \tag{13}$$

where Π_0 stands for $[\![\phi_0]\!]_{TE}$, and $\Pi(y')=\Pi_0(y')+\mathcal{R}_1^2[\![\varphi+\varphi_H^P]\!]_{TE}$.

Outer Problem and Matching

In the flow region removed from the wing sections, the spatial variation is scaled by b, and the solution may be represented to the leading order by concentrated vortices with circulation $\Gamma_0(y)$ bounded to the centerline together with the trailing vortex sheet. The perturbation potential for this outer problem is then $\Phi=\Phi_0+\mathcal{R}_1^{-1}\Phi_1+\ldots$, with

$$\Phi_0(x,y,z) = \frac{1}{4\pi}\int_{-1}^{1}\frac{\Gamma_0(y_1)}{(y-y_1)^2+z^2}\times\left[1+\frac{x-my_1}{|(x-my_1)^2+(y-y_1)^2+z^2|^{1/2}}\right]\mathrm{d}y_1 \tag{14}$$

In approaching the centerline, Φ_0 can be expanded for small $\xi\equiv x-my$ and z; through transformation Eqs. (1) and observing that $\Gamma_0(y)=\Gamma_0(y'\cos\Lambda)-2m\mathcal{R}_1^{-1}x'\mathrm{d}\Gamma_0/\mathrm{d}y'$; this inner limit can be obtained as

$$\Phi \sim (2\pi)^{-1}\Gamma_0(y'\cos\Lambda)\left[\tan^{-1}\left(\frac{x'}{z'}\right)+\frac{\pi}{2}\mathrm{sgn}z'\right] - (\pi)^{-1}m\mathcal{R}_1^{-1}x'\left(\frac{\mathrm{d}\Gamma_0}{\mathrm{d}y'}\right)\left[\tan^{-1}\left(\frac{x'}{z'}\right)+\frac{\pi}{2}\mathrm{sgn}z'\right] + (\pi)^{-1}m\mathcal{R}_1^{-1}z'\left(\frac{\mathrm{d}\Gamma_0}{\mathrm{d}y'}\right)\ln|\zeta| + 2\mathcal{R}_1^{-1}z'\Sigma(y) + O(\mathcal{R}_1^{-2}|\zeta|^2,\zeta^{-1},\mathcal{R}_1^{-1}) \tag{15a}$$

where $\Sigma(y)$ is the upwash function in y (not y')

$$\Sigma(y) \equiv -(2\pi)^{-1}\sin\Lambda\Gamma_0'(y)\ln(\mathcal{R}_1) + (4\pi)^{-1}\Gamma_0'(y)\left[\ln\left|\frac{1-y}{1+y}\frac{(1+\sin\Lambda)^2}{\cos^2\Lambda}\right| - \sin\Lambda\left(2+\ln\left|\frac{1-y^2}{\cos^2\Lambda}\right|\right)\right] + (4\pi)^{-1}\int_{-1}^{1}\frac{\Gamma_0'(y_1)-\Gamma_0'(y)}{y_1-y}[1-\sin\Lambda\,\mathrm{sgn}(y_1-y)]\mathrm{d}y_1 \tag{15b}$$

where $\Gamma_0'(y)\equiv\mathrm{d}\Gamma_0/\mathrm{d}y$. Equations (13) and (15) are valid expansions in $\mathcal{R}_1^{-1}$ in the common domain $1\ll|\zeta|\ll\mathcal{R}_1$, where the inner and outer solutions are matched, after making the identifications

$$\Gamma_0(y'\cos\Lambda)=\Pi_0(y'), \quad V_1^\infty=2\Sigma(y) \tag{16}$$

The upwash correction, hence, the inner solution to the order $\mathcal{R}_1^{-1}$, is now determined.

Comparisons with Other Solutions

In the following, comparisons are made of the present analysis with exact solutions derived from an inverse method and with results from a panel method.

Uniformly Loaded Oblique Wings

Wing upwash (slope) supporting a given lift distribution can be determined with relative ease; for a uniform distribution, the task reduces to evaluating a line integral. Upwash calculation has been made for several planforms with uniform load in this manner to furnish a basis for assessing the theory. Using the upwash data as input, $[\![C_p']\!]$ are computed by the present theory and then compared to the exact (uniform) load. This provides a test of the theory as a direct method. Of all examples considered with $\mathcal{R}_0 \equiv 2\ell/c_0 = 10$ to 40 and $\Lambda = 0$ to 45 deg, a useful feature is that, over most parts of the wing, the upwash can be very closely represented by (with $c' \equiv b' - a'$)

$$\left[A(y') + \frac{x'-a'}{c'} B(y')\right] \ell n\left(\frac{b'-x'}{x'-a'}\right) + C(y') \qquad (17)$$

where B and C are generally small and decrease with increasing aspect ratio. This fact is utilized to expedite to the $[\![C_p']\!]$ computation. Figure 2 presents chordwise lift distributions at several spanwise stations computed from such an upwash over a 20:1 elliptic planform at 26.6 deg yaw, for which the exact $-[\![C_p']\!]$ has a normalized value unity. Good agreement with the exact value (unity) is seen at the inboard spanwise stations, with maximum error occurring near LE of less than 3%. This represents a great improvement over the strip theory (not shown) which has an error of typically 6 to 18%. Near the tips ($|y'/\ell| \to 1$), the lifting-line solution deteriorates, as expected. At the 80% station (dash curves), signs of breakdown appear near the LE, which are partly caused by inadequacy of curve fitting based on Eq. (17) near the tip. However, the span loading (not shown) appears to remain satisfactory even at the 80% span station. Other examples with lower aspect ratio ($\mathcal{R}_l = 10$), a larger sweep ($\Lambda = 45$ deg), as well as nonuniform lift distributions, have been studied; except for a slightly large discrepancy near the tips, similar conclusions can be drawn for those cases.

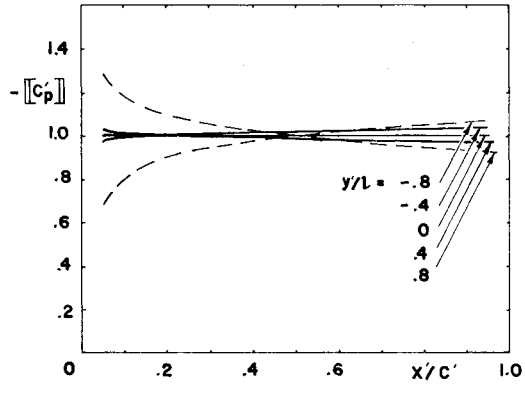

Fig. 2 Comparison of present theory with exact solution in chordwise lift distribution at various span stations. The lifting surface has a 20:1 elliptic planform at 26.6 deg yaw; exact solution is $-[\![C_p]\!] = 1$.

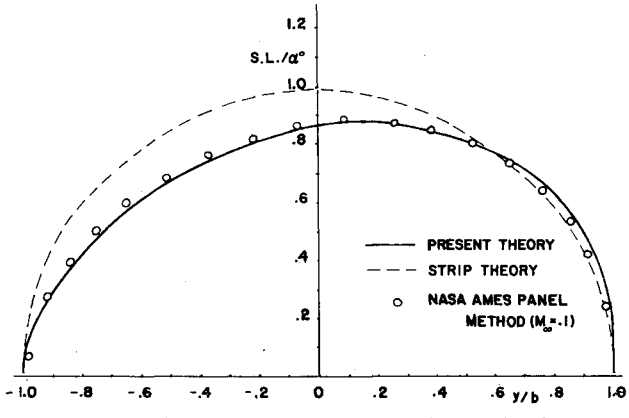

Fig. 3 Span loading of an elliptic flat plate with a ratio of unyawed span to root-chord 16.78 and a straight 40% chord line at 45 deg yaw.

Oblique Flat Wings

Vortex-lattice and wing-panel methods have proven adequate in many linear lifting-surface problems,[7,8] but their application to oblique wings does not appear to exist in the literature. The data by panel method used in the following comparison (provided by R. Smith) are generated from a computer program developed at NASA Ames Research Center, based on an extension of Woodward's method applied originally to symmetric planforms.[8] Figure 3 presents a comparison in span loading for an elliptic flat-plate wing of $\mathcal{R}_0 = 16.78$ with a straight 40% chord line at 45 deg yaw. For elliptic flat plates, the theory gives a span loading in terms of elementary functions

$$SL/8\cos\Lambda\alpha = \sqrt{1-y^2}\cdot\left(1-\frac{\pi}{2\mathcal{R}_l}\right) - \frac{\sin\Lambda}{\mathcal{R}_l}\sqrt{1-y^2}\sin^{-1}y + \frac{\sin\Lambda}{\mathcal{R}_l}\cdot y\cdot\left\{\ell n(8\mathcal{R}_l\sqrt{1-y^2}) - (1-2k) - csc\Lambda[\ell n\,|1+\sin\Lambda| - (1-\sin\Lambda)\ell n\,|\cos\Lambda|]\right\} \qquad (18)$$

where α is the angle of attack, k is the straight-axis location in fraction of chord. As clearly shown, the difference between the present theory (solid line) and the panel method (open circles) is small at most stations as compred to either of their differences from the (uncorrected) strip theory (dashed line). Good agreement with the panel method is also found in a comparison made for an ESP (extended-span-planform) wing[5,9] (not shown).

Acknowledgment

The study is supported by the Office of Naval Research under Contract N00014-75-C-0520; partial support on an earlier joint study with NASA Ames Research Center Aeronautics Division (NCA2-OR-730-601) is also acknowledged. Thanks are due to S. Y. Meng for devising a method for computing the upwash function and L. Murillo for producing the exact solutions and many results in the comparison study. Helpful discussions with R.T. Jones and R. Smith at NASA Ames Research Center are much appreciated.

References

[1] Prandtl, L., "Tragflügel Theorie" *Nachrichten d.k. Gesellschaft d. Wiss. zu Göttingen,* Math-Phys. Klasse, 1918, pp. 451-477.

[2] Van Dyke, M. D., *Perturbation Methods in Fluid Mechanics*, Academic Press, New York, 1964, pp. 167-176.

[3] Ashley, H. and Landahl, M., *Aerodynamics of Wings and Bodies*, Addison-Wesley, Mass., 1965, pp. 137-142.

[4] Cheng, H. K., "On Lifting-Line Theory in Unsteady Aerodynamics," University of Southern California, School of Engineering, Dept. of Aerospace Engineering, Rept. USCAE 133, 1976.

[5] Cheng, H. K., "Theory of Oblique Wings of High Aspect Ratio," University of Southern California, School of Engineering Dept. of Aerospace Engineering, Rept. USCAE 135, Aug. 1978.

[6] Jones, R. T., "The Oblique Wing—Aircraft Design for Transonic and Low Supersonic Speeds," *Acta Astronautica*, Vol. 4, 1977, pp. 99-100.

[7] Ashley, H. and Rodden, W., "Wing-Body Aerodynamic Interaction," *Annual Review of Fluid Mechanics*, Vol. 4, 1972, pp. 431-472.

[8] Woodward, F. A., "An Improved Method for the Aerodynamic Analysis of Wing-Body-Tail Configurations in Subsonic and Supersonic Flow," NASA CR-2228, Pts. I and II, May 1973.

[9] Black, R. L., Beamish, J. K., and Alexander, W. K., "Wind Tunnel Investigation of a Oblique Wing Transport Model at Mach Number Between 0.6 and 1.4," NASA CR-137697, HST-TR-344-0, July 1975, p. 11.